

# Molecular Cancer Research



## Ligand Binding Promotes CDK-Dependent Phosphorylation of ER-Alpha on Hinge Serine 294 but Inhibits Ligand-Independent Phosphorylation of Serine 305

Jason M. Held, David J. Britton, Gary K. Scott, et al.

*Mol Cancer Res* 2012;10:1120-1132. Published OnlineFirst June 5, 2012.

**Updated version** Access the most recent version of this article at:  
doi:[10.1158/1541-7786.MCR-12-0099](https://doi.org/10.1158/1541-7786.MCR-12-0099)

**Supplementary Material** Access the most recent supplemental material at:  
<http://mcr.aacrjournals.org/content/suppl/2012/06/05/1541-7786.MCR-12-0099.DC1.html>

**Cited Articles** This article cites by 40 articles, 15 of which you can access for free at:  
<http://mcr.aacrjournals.org/content/10/8/1120.full.html#ref-list-1>

**E-mail alerts** [Sign up to receive free email-alerts](#) related to this article or journal.

**Reprints and Subscriptions** To order reprints of this article or to subscribe to the journal, contact the AACR Publications Department at [pubs@aacr.org](mailto:pubs@aacr.org).

**Permissions** To request permission to re-use all or part of this article, contact the AACR Publications Department at [permissions@aacr.org](mailto:permissions@aacr.org).

## Ligand Binding Promotes CDK-Dependent Phosphorylation of ER-Alpha on Hinge Serine 294 but Inhibits Ligand-Independent Phosphorylation of Serine 305

Jason M. Held<sup>1</sup>, David J. Britton<sup>1</sup>, Gary K. Scott<sup>1</sup>, Elbert L. Lee<sup>1</sup>, Birgit Schilling<sup>1</sup>, Michael A. Baldwin<sup>1</sup>, Bradford W. Gibson<sup>1,2</sup>, and Christopher C. Benz<sup>1,3</sup>

### Abstract

Phosphorylation of estrogen receptor- $\alpha$  (ER $\alpha$ ) is critical for its transcription factor activity and may determine its predictive and therapeutic value as a biomarker for ER $\alpha$ -positive breast cancers. Recent attention has turned to the poorly understood ER $\alpha$  hinge domain, as phosphorylation at serine 305 (Ser305) associates with poor clinical outcome and endocrine resistance. We show that phosphorylation of a neighboring hinge domain site, Ser294, analyzed by multiple reaction monitoring mass spectrometry of ER $\alpha$  immunoprecipitates from human breast cancer cells is robustly phosphorylated exclusively by ligand (estradiol and tamoxifen) activation of ER $\alpha$  and not by growth factor stimulation (EGF, insulin, heregulin- $\beta$ ). In a reciprocal fashion, Ser305 phosphorylation is induced by growth factors but not ligand activation of ER $\alpha$ . Phosphorylation at Ser294 and Ser305 is suppressed upon co-stimulation by EGF and ligand, respectively, unlike the N-terminal (AF-1) domain Ser118 and Ser167 sites of ER $\alpha$  where phosphorylation is enhanced by ligand and growth factor co-stimulation. Inhibition of cyclin-dependent kinases (CDK) by roscovitine or SNS-032 suppresses ligand-activated Ser294 phosphorylation without affecting Ser118 or Ser104/Ser106 phosphorylation. Likewise, cell-free studies using recombinant ER $\alpha$  and specific cyclin-CDK complexes suggest that Ser294 phosphorylation is primarily induced by the transcription-regulating and cell-cycle-independent kinase CDK7. Thus, CDK-dependent phosphorylation at Ser294 differentiates ligand-dependent from ligand-independent activation of Ser305 phosphorylation, showing that hinge domain phosphorylation patterns uniquely inform on the various ER $\alpha$  activation mechanisms thought to underlie the biologic and clinical diversity of hormone-dependent breast cancers. *Mol Cancer Res*; 10(8); 1120–32. ©2012 AACR.

### Introduction

As a member of the nuclear hormone receptor family, estrogen receptor- $\alpha$  (ER $\alpha$ ) plays a complex and diverse role in orchestrating such organ-specific functions as mammary gland development, bone homeostasis, and cardiovascular vitality (1). The varied physiologic mechanisms driven by this sex steroid receptor are primarily initiated by its high-affinity binding to an endogenous estrogenic ligand, 17-

$\beta$ -estradiol (E2), which triggers both nongenomic (membrane-based protein interactions) and genomic (nuclear-based DNA interactions) receptor responses (2). In the context of nearly 70% of newly diagnosed human breast cancers, the full-length 67-kDa ER $\alpha$  protein is transcriptionally and translationally overexpressed, driving both preneoplasia and invasive tumor growth and metastasis (2). This key role of ER $\alpha$  in promoting the development and clinical progression of breast cancer explains the impressive clinical success of ligand-targeted antiestrogenic therapeutics (e.g., tamoxifen, aromatase inhibitors) in both preventing and treating ER-positive breast cancer (2).

Despite the clinical success of antiestrogenic agents, 30% to 50% of ER-positive breast cancers exhibit either *de novo* or acquired resistance to ligand-targeted therapeutics, yet at least 80% of these resistant tumors retain their receptor overexpression and dependence on ER $\alpha$  genomic and nongenomic activities (3). Understanding the molecular mechanisms promoting antiestrogen resistance and breast cancer escape from ER $\alpha$  ligand dependence has been challenging, leading to the emergence of receptor cross-talk as a mechanistic paradigm wherein growth factor-activated cell signaling pathways converge to structurally alter ER $\alpha$  protein in such a way as to activate its genomic and nongenomic

**Authors' Affiliations:** <sup>1</sup>The Buck Institute for Research on Aging, Novato; <sup>2</sup>Department of Pharmaceutical Chemistry, and <sup>3</sup>Department of Medicine and Division of Oncology-Hematology, University of California, San Francisco, California

**Note:** Supplementary data for this article are available at Molecular Cancer Research Online (<http://mcr.aacrjournals.org/>).

J.M. Held and D.J. Britton made equal contributions to this work.

Current address for D.J. Britton: Proteome Sciences plc, Institute of Psychiatry, King's College, De Crespigny Park, London SE5 8AF, UK.

**Corresponding Author:** Christopher C. Benz, Buck Institute for Research on Aging, 8001 Redwood Blvd, Novato, CA 94945. Phone: 415-209-2092; Fax: 415-209-2232; E-mail: [cbenz@buckinstitute.org](mailto:cbenz@buckinstitute.org)

doi: 10.1158/1541-7786.MCR-12-0099

©2012 American Association for Cancer Research.

functions, even in the absence of ligand (3, 4). This paradigm of ligand-independent ER $\alpha$  activation by cross-talking signal transduction pathways extends to other members of the ligand-binding hormone receptor family (5) and builds upon more than a decade of evidence that such receptors are subject to a constellation of structurally significant and functionally important posttranslational modifications (PTM) which occur throughout the receptor protein either in the presence or in the absence of bound ligand. With regard to ER $\alpha$ , phosphorylation (on serine, threonine, or tyrosine residues) is the most common and best studied, although ER $\alpha$  PTMs also include acetylation, methylation, SUMOylation, and ubiquitination (2). While the functional and clinical consequences of these various ER $\alpha$  PTMs remain largely obscure, recent identification of protein kinases linked to specific ER $\alpha$  phosphorylation sites, including those capable of transcriptionally activating ER $\alpha$  in the absence of ligand (2, 3), have stimulated interest in growth factor signaling pathways potentially associated with antiestrogen resistance mechanisms that may be therapeutically targeted by small-molecule kinase inhibitors (3).

Early studies identified several serine residues in the N-terminal activation function 1 domain (AF-1) of ER $\alpha$ , most prominently Ser118 and Ser167, as being phosphorylated with receptor activation in ER-positive breast cancer cells exposed to ligand or growth factors (2, 6). Limited retrospective clinical studies using antibodies to interrogate ER $\alpha$  phosphorylation at either Ser118 or Ser167 in archived primary breast tumors with known responsiveness to tamoxifen therapy have either shown no significant response association or a surprising correlation with increased tamoxifen sensitivity (2, 6–8). However, recent attention has focused on the ER $\alpha$  hinge domain where phosphorylation at Ser305 appears to be correlated with antiestrogen resistance (9–12). The ER $\alpha$  hinge domain is a short, flexible region linking the ligand binding and activation 2 domain (LBD/AF-2) with the DNA-binding domain (DBD) and is thought to play an important role facilitating conformational synergy between the LBD/AF-2 and the AF-1 domains following ligand binding (13). Only 60 amino acids in length, the hinge domain can become highly decorated by acetylation (14), ubiquitination (15), SUMOylation (16), or methylation (17) in addition to phosphorylation, suggesting that PTMs play an important regulatory role in ER $\alpha$  activation.

Our recent mass spectrometry screen for ER $\alpha$  PTMs revealed a novel hinge domain phosphorylation site at Ser294, present in E2-exposed MCF-7 cells, a human breast cancer cell line (18). While early investigations into ER $\alpha$  residues targeted for phosphorylation had considered Ser294 a potential candidate given its association with a proline-directed kinase motif (19), more extensive studies have been hampered by the lack of facile methods to interrogate Ser294 phosphorylation. Nonetheless, very recent studies in addition to results presented here have shown that Ser294 is, in fact, phosphorylated in response to ligand and that this phosphorylation is required for full transcriptional activity by ER $\alpha$  (18, 20). In this report, we

use multiple reaction monitoring mass spectrometry (MRM/MS) to quantitatively evaluate the endogenous induction of Ser294 phosphorylation within various ER-positive breast cancer models and show that robust Ser294 phosphorylation occurs exclusively upon ligand stimulation (E2 or tamoxifen) and not following growth factor stimulation (EGF, insulin, heregulin- $\beta$ ) of ER $\alpha$ , unlike phosphorylation occurring at Ser118, Ser167, or Ser305. These quantitative MRM/MS findings are independently validated by immunoassay using a newly generated anti-pSer294 polyclonal antibody. Moreover, specific comparison of hinge phosphorylation at Ser294 and Ser305 reveals not only their reciprocal responsiveness to ligand-dependent versus ligand-independent ER $\alpha$  activation but also their reciprocal blunting of phosphorylation upon combined ligand and growth factor stimulation, suggesting that the hinge domain acts as a specific readout for the mode of ER $\alpha$  activation as well as a sensor of receptor cross-talk. Finally, treatment of cells with small-molecule cyclin-dependent kinase (CDK) inhibitors as well as cell-free assays using recombinant ER $\alpha$  and specific cyclin-CDK complexes show that the subset of transcription-regulating and cell-cycle-independent kinases, most prominently CDK7, mediate ligand-dependent phosphorylation of Ser294 without affecting other ER $\alpha$  phosphorylation sites including Ser118, Ser104, or Ser106. This observation is made therapeutically relevant by the clinical advancement of specific inhibitors of this CDK7 subclass.

## Materials and Methods

### Cell culture and reagents

The human breast cancer cell lines MCF-7, BT474, and T47D were originally obtained from American Type Culture Collection and were grown under American Type Culture Collection–recommended conditions: 37°C, 5% CO<sub>2</sub> and in Dulbecco's Modified Eagle's Medium (DMEM), McCoy's 5A, or RPMI-1640 media supplemented with 10% FBS, 1% penicillin/streptomycin. (Mediatech, Inc.) We obtained phenol red-free DMEM supplemented with L-glutamine and recombinant EGF and ER $\alpha$  from Invitrogen; charcoal-stripped serum (CSS) from Hyclone (Thermo Scientific);  $\beta$ -estradiol, 4-hydroxytamoxifen (TAM), okadaic acid, forskolin, insulin heregulin- $\beta$ , and IGEPAL CA-630 from Sigma-Aldrich; ER $\alpha$  antibody (clone F-10) from Santa Cruz Biotechnology; pSer118 and pSer167 monoclonal antibodies from Cell Signaling; pSer104/pSer106 rabbit monoclonal antibody from Epitomics; and pSer305 rabbit monoclonal antibody (clone 124.9.4) from Millipore.

### ER $\alpha$ transfection assays

Full-length ER $\alpha$  cloned into the pSG5 expression vector (gift of Paul Webb, UCSF, San Francisco, CA) was used to produce wild-type ER $\alpha$ , whereas expression of the Ser294-Ala ER $\alpha$  mutant from pSG5 was obtained by replacing a unique *NotI*-*HindIII* fragment containing the Ser294 codon with the corresponding fragment containing the Ser294Ala

mutation (Ser294Ala ER $\alpha$  mutant plasmid, gift of Susan Fuqua, Baylor College of Medicine, Houston, TX). Both ER $\alpha$  wild-type and Ser294Ala mutant plasmids were verified by sequencing. To achieve approximately 3 times endogenous ER $\alpha$  levels,  $4 \times 10^5$  MCF-7 cells plated into 60-mm dishes were transfected with 0.5  $\mu$ g of pSG5 wild-type ER $\alpha$ , pSG5 Ser294 mutant ER $\alpha$ , or the empty vector pSG5 using Lipofectamine 2000 from Invitrogen in DMEM for 6 hours. The media were then replaced with medium supplemented with 10% FBS for an additional 18 hours after which time the media were replaced with phenol red-free DMEM:H-16 supplemented with 10% CSS. Following 36 hours in the phenol red-free CSS, cells were either treated with 10 nmol/L E2 or left untreated for an additional 6 hours after which cells were harvested for total cell lysates or RNA using TRIzol from Invitrogen. Experiments were repeated 3 times with each experiment using two 60-mm dishes per condition per vector.

#### Semiquantitative reverse-transcription PCR

Total RNA was harvested using TRIzol followed by treatment with DNA-free (Ambion) according to the manufacturer's specifications to remove potentially contaminating DNA. Reversed transcription was conducted using oligo

(dT) priming of 0.5  $\mu$ g RNA per sample condition with SuperScript II (Invitrogen) according to manufacturer's specifications. PCR reactions used 1- $\mu$ L aliquots from the reverse-transcription (RT) reactions with Pfu polymerase (New England Biolabs). Reaction conditions consisted of annealing at 60°C for 30 seconds, extension at 72°C for 25 seconds, and denaturation at 96°C for 10 seconds with identically prepared reactions subjected to 24, 26, or 28 PCR cycles. PCR products were electrophoresed on 8% PAGE, stained with ethidium bromide, photographed and quantified by densitometry using a GS-710 Calibrated Imaging Densitometer (Bio-Rad). Error bars on Fig. 1B represent the SD of gel-stained intensities normalized by the respective glyceraldehyde-3-phosphate dehydrogenase (GAPDH) intensity from the 3 separate transfection experiments. Validation of statistical difference was conducted using a *t* test (2-sample assuming unequal variance) with asterisks indicating significant reductions ( $P < 0.05$ ) in the Ser294Ala levels relative to E2-stimulated empty vector levels and wild-type ER $\alpha$  levels. Primers include AREG (amphiregulin; 170 bp): 5'aaaaggaggaggcaaaatgg3' (forward), 5'tcatggacttttccccaca3' (reverse); EGR3 (238 bp): 5'gcagcatggtcttctgactgaa3' (forward), 5'cccccttccactagatcc3' (reverse); CXCL12 (221 bp): 5'tagtcaagtgcgtccacga3' (forward) 5'ggacacaccacagca-

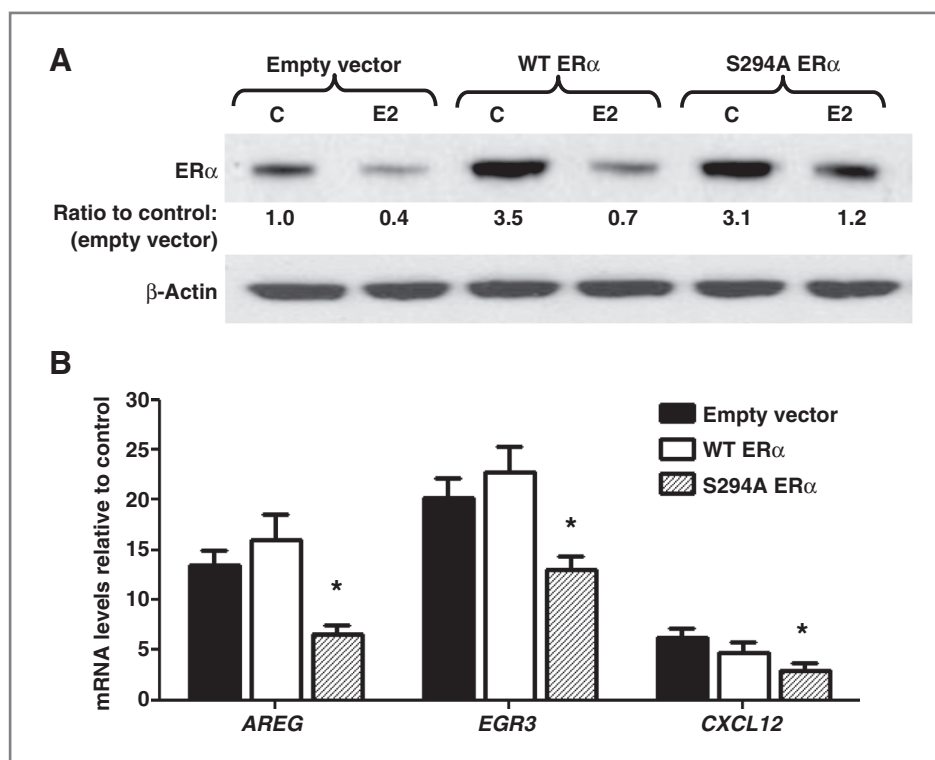


**Figure 1.** MCF-7 cells transfected with an Ser294Ala-mutated ER $\alpha$  expression construct produce transcriptional suppression of E2-inducible genes. A, immunoblot analysis of ER $\alpha$  protein levels in MCF levels following transfection with empty vector, exogenous wild-type (WT) ER $\alpha$ , or Ser294Ala ER $\alpha$  in the absence (C) or presence (E2) of 10 nmol/L E2 for 6 hours. Note the similar degree of ER $\alpha$  downregulation following E2 stimulation relative to basal levels in all 3 transfection sets. Equal protein loading was confirmed by probing for  $\beta$ -actin. B, quantitation of gene transcript levels by densitometry of PCR products visualized with ethidium. Levels of 3 E2-inducible genes (AREG, EGR3, CXCL12) are normalized relative to empty vector control levels (set equal to 1.0) with all gene transcripts levels originally normalized by their respective GAPDH. Error bars represent SD of densitometric quantifications obtained from 3 biologic replicates. \*, significant reductions ( $P < 0.05$ ) in the Ser294Ala inductions relative to E2-stimulated empty vector and WT ER $\alpha$  transfectants as assessed by the Student *t* test (2-way, unpaired). See Materials and Methods for specific gene primers.



caaac3' (reverse); and GAPDH (234 bp): 5'cgaattggctaca-gcaacagg3' (forward), 5'gtacatgacaaggtcggctc3' (reverse).

### Cell culture treatment conditions and ER $\alpha$ immunoprecipitation

Twenty-four hours before ER $\alpha$  isolation, the standard cell growth media were removed, the cells washed 3 times with PBS (room temperature) and replaced with phenol red-free DMEM with or without 10% CSS depending upon treatment conditions. The various E2 and growth factor treatment regimens are detailed in appropriate figure legends and the Results section. Following treatment, the cells were washed once with room-temperature PBS before harvesting on ice using a cell scraper with 1.0 mL of ice-cold cell lysis buffer [100 mmol/L NaCl, 20 mmol/L Tris (pH 7.5), 0.5% IGEPAL-630, 100 mmol/L NaF, 10 mmol/L Na<sub>3</sub>VO<sub>4</sub>, 50 mmol/L Na<sub>2</sub>MoO<sub>4</sub>, 1 tablet/10 mL PhosSTOP (Roche Applied Science), 320 nmol/L okadaic acid, and 1 tablet/10 mL Roche mini-complete protease inhibitor cocktail (Roche Applied Science)] per one 15-cm plate of cells. The cellular lysate was then sonicated twice for 10 seconds while on ice and then centrifuged at 16,000 rpm (15 minutes, 4°C). ER $\alpha$  from the resulting cleared supernatant was immunoprecipitated by the addition of 8  $\mu$ L of ER $\alpha$  antibody (1.6  $\mu$ g, F-10; Santa Cruz Biotechnology) together with 15  $\mu$ L Protein G Sepharose 4 Fast Flow beads (GE Healthcare) and incubated with slow rotation at 4°C for 6 hours. The beads were then pelleted at 2,500 rpm for 1 minute, the supernatant was removed, and the beads were washed 3 times in wash buffer (125 mmol/L NaCl, 20 mmol/L Tris, pH 7.5, and 0.35% IGEPAL).

### Western blot analysis

Aliquots of the immunoprecipitated ER $\alpha$  from the breast cancer cells were analyzed by Western blotting as previously described (21). Briefly, samples were run on NuPAGE 4% to 12% gels (Invitrogen), transferred to polyvinylidene difluoride (PVDF) Immobilon-P membranes (Millipore), with membranes then blocked and probed using 4% nonfat dry milk power dissolved in TBS with Tween (TBST; 150 mmol/L NaCl, 50 mmol/L Tris, pH 7.5, and 0.05% Tween). Membranes were incubated with primary antibodies for 2 hours at room temperature, washed in TBST, and then incubated with a horseradish peroxidase (HRP)-coupled secondary antibody. Washed membranes were developed using SuperSignal West Pico Chemiluminescent Substrate (Thermo Scientific).

### pSer294 antibody generation

Four rabbits were immunized with a synthetic phosphopeptide corresponding to residues surrounding pSer294 of ER $\alpha$  according to the vendor's protocols (Epitomics). Following immunization, the antisera were separately evaluated by Western blot analysis using immunoprecipitated ER $\alpha$  where the pSer294 levels had been previously validated by MS. The antiserum from one rabbit was particularly successful by Western blot analysis in recapitulating the MS results for pSer294 levels. However, as MS results consistently

detect no difference, or even a slight decrease, in pSer294 levels between control and EGF-stimulated ER $\alpha$ , the slight (~4%) increase in reactivity of this pSer294 antisera to EGF-stimulated ER $\alpha$  versus control ER $\alpha$  suggest slight residual cross-reactivity to epitopes other than pSer294. Splenocytes from this rabbit are currently being used in the development of a pSer294 monoclonal antibody (Epitomic).

### On-bead proteolytic digestion

To avoid electrophoretic separation and in-gel ER $\alpha$  digestion before MS, ER $\alpha$  immunoprecipitates were trypsin-digested while complexed to the sepharose beads as previously described (18). The samples were not reduced or alkylated. Aliquots of the washed bead-bound immune complexes were transferred to siliconized 1.5 mL microcentrifuge tubes and washed twice in 100 mmol/L Tris (pH 7.0) and 3 times in 25 mmol/L NH<sub>4</sub>HCO<sub>3</sub> by gentle rotation for 2 minutes at room temperature. One hundred and fifty microliters of NH<sub>4</sub>HCO<sub>3</sub> was added to the pelleted beads, followed by addition of 400 ng sequencing grade trypsin (23  $\mu$ L of 17 ng/ $\mu$ L stock solution; Promega) and then left to incubate overnight at 37°C with shaking at 950 rpm in an Eppendorf Thermomixer. Microcentrifuge tubes were centrifuged at 12,000 rpm, and the peptide solution carefully transferred (to avoid carryover of the beads) to low-binding polymer technology 0.65 mL microcentrifuge tubes (PGC Scientific). Ten microliters of acetonitrile and 1  $\mu$ L of 10% formic acid were added, and the peptide solution was concentrated to approximately 15  $\mu$ L. Each sample was divided into three 5- $\mu$ L aliquots and stored at -80°C until used for MS.

### Synthesis of stable isotope-labeled SER167 and SER294 peptides

Stable isotope-labeled and -unlabeled peptides corresponding to the unmodified and phosphorylated tryptic peptides quantified by MRM for Ser167 and Ser294 were synthesized by Cambridge Peptides Ltd. using Fmoc solid phase peptide chemistry and purified using reverse-phase high-performance liquid chromatography (HPLC). Peptides were purified to 90% to 98% purity, each resulting in 2 to 3 mg of lyophilized peptide. The peptide sequences and isotope information are listed in Table 1.

Each peptide was solubilized using 5% acetonitrile, 0.1% formic acid in a volume resulting in peptide concentrations of approximately 1 mmol/L. Peptides were divided into 100  $\mu$ L aliquots and stored at -80°C. One aliquot was shipped on dry ice for amino acid analysis to accurately determine the peptide concentrations. Amino acid analysis was conducted at the Protein & Nucleic Acid Chemistry Facility (PNAC), Department of Biochemistry, University of Cambridge (Cambridge, UK). Peptides were then diluted to suitable concentrations according to the instrument parameter optimization experiments (10 pmol/ $\mu$ L; direct infusion), calibration curves (0.005–50 fmol/ $\mu$ L), internal standards of ER IP/digests (5 fmol/ $\mu$ L).

**Table 1.** Stable isotope-labeled peptides synthesized

Peptide name	Amino acid sequence	Stable isotope label
Heavy SER167	LASTNDKGSMAMESAK	K, U-13C6; 15N2
Light SER167	LASTNDKGSMAMESAK	
Heavy pSER167	LASTNDKGSMAMESAK	K, U-13C6; 15N2
Light pSER167	LASTNDKGSMAMESAK	
Heavy SER294	AANLWPSPLMIK	K, U-13C6; 15N2
Light SER294	AANLWPSPLMIK	
Heavy pSER294	AANLWPSPLMIK	K, U-13C6; 15N2
Light pSER294	AANLWPSPLMIK	

NOTE: Synthetic stable isotope-labeled and -unlabeled peptides used to generate a calibration curve and measure absolute levels of phosphorylated and unmodified Ser167 and Ser294 of ER $\alpha$  with an SID-MRM assay. The underlined K indicates the position of the heavy-labeled lysine and the underlined S indicates the phosphorylation site in each peptide.

### NanoLC-MRM/MS analysis

To quantify relative changes in ER $\alpha$  Ser167 and Ser294 phosphorylation levels by MRM/MS, ER $\alpha$  immunoprecipitates were analyzed by nanoLC-MRM/MS on a 4000 QTRAP hybrid triple quadrupole/linear ion trap mass spectrometer (AB Sciex) as previously described (18) and further detailed in the Supplementary Methods. To compare the relative levels of phosphorylated Ser294 and Ser167 in different samples, the MRM peak area of the phosphorylated peptide was divided by the unmodified peptide peak area for normalization to total ER $\alpha$  levels and is referred to as the "phosphorylated:unmodified peptide area ratio." S-lens and Q2 collision energy optimization for the TSQ Vantage are described in the Supplementary Methods.

### Stable isotope dilution-MRM assay for absolute quantification of endogenous ER $\alpha$ tryptic peptides

To determine the molar amount of endogenous ER $\alpha$  by stable isotope dilution (SID)-MRM, following immunoprecipitation of ER and on-bead digestion, the peptide solution was removed from the beads and 10  $\mu$ L of 50% acetonitrile, 5% formic acid was added. Samples were dried in a Speedvac and resolubilized in 25  $\mu$ L of 3% acetonitrile, 0.2% formic acid containing 5 fmol/ $\mu$ L of each stable isotope-labeled peptide, in addition to 200  $\mu$ g/mL glucagon to improve peptide stability. An 8- $\mu$ L aliquot of each sample was analyzed per injection on a TSQ Vantage with detailed LC-MS instrument settings listed in the Supplementary Methods.

### Normal response curves

A response curve was generated for each peptide to determine assay characteristics including the linear range of the assay, limits of detection (LOD), and limits of quantification (LOQ). The Supplementary Methods describe how the peptide response curves were generated. The LOD was calculated from the variance of the blank sample with no peptides spiked in and the variance of the lowest spiked in concentration (lowest values shown in the table in Supplementary Methods) as previously described (22). Assuming a

type I error rate  $\alpha = 0.05$  for deciding that the peptide is present when it is not and a type II error rate  $\beta = 0.05$  for not detecting the peptide when it is present, LOD was calculated with:

$$\text{LOD} = \frac{\text{mean}_b + t_{1-\beta} \times (\text{SD}_b + \text{SD}_s)}{2}$$

Where the  $t_{1-\beta}$  term is equal to the  $(1 - \beta)$  percentile of the standard  $t$  distribution on  $n$  degrees of freedom, where  $n$  is equal to the number of replicates. LOD values were then transformed and calculated into concentrations using the linear regressions described above. This method relies on the LOD being in a region of the regression where the response is still linear. Once the LOD was determined, the LOQ was calculated using the customary relation of  $\text{LOQ} = 3 \times \text{LOD}$ .

### In vitro CDK assays

Five picomoles of recombinant ER $\alpha$  was incubated with 200 ng of the indicated CDK (SignalChem) at 30°C for 60 minutes in 10 mmol/L MgCl<sub>2</sub>, 60 mmol/L HEPES, pH 7.4, 1.2 mmol/L dithiothreitol (DTT), and 100  $\mu$ mol/L ATP with a total reaction volume of 30  $\mu$ L. CDK-cyclin pairs used were CDK1-cyclinA1, CDK2-cyclinA2, CDK4-cyclinD1, CDK7-cyclinH1/MNAT1, and CDK9-cyclinK. Aliquots were then analyzed for pSer294 by Western blotting or MRM/MS.

## Results

### Functional analysis of Ser294 phosphorylation using a dominant-negative strategy

As a previous study had shown the requirement of Ser294 phosphorylation to drive ER $\alpha$  transcriptional activity in an ER $\alpha$ -null cell line (20), a dominant-negative strategy was used to determine the functional relevance of pSer294 to ER $\alpha$  transcriptional activity in the context of an ER $\alpha$ -positive cell line. Thus, MCF-7 cells were transiently transfected with an ER $\alpha$  expression construct containing a Ser294Ala mutation. As a control, MCF-7 cells were

transiently transfected with a wild-type ER $\alpha$  expression construct or empty vector (pSG5). The level of exogenous ER $\alpha$  introduced into the MCF-7 cells by the mutant and wild-type expression constructs was approximately 3-fold above endogenous (empty vector) ER $\alpha$  levels as determined by densitometry of Western blotting (Fig. 1A). Following 6 hours of stimulation with E2, we observed the anticipated downregulation of ER protein (2.5- to 3-fold) in all conditions, which is consistent with normal proteasomal degradation of ER $\alpha$  following its E2-induced transcriptional activation (Fig. 1A; ref. 23). To evaluate the influence of the Ser294Ala-mutated ER $\alpha$  upon E2-dependent gene transcription, we used semiquantitative RT-PCR to measure the induction of 3 genes (amphiregulin, *AREG*; early growth response 3, *EGR3*; and chemokine ligand 12, *CXCL12*) previously known to be highly E2-inducible in MCF-7 cells following 8 hours of E2 stimulation (24, 25). As seen in Fig. 1B, all 3 of these genes showed significantly reduced (30%–50%) E2 induction in the Ser294Ala ER $\alpha$ -overexpressing MCF-7 cells relative to MCF-7 cells transfected with either wild-type ER $\alpha$  or empty vector ( $P < 0.05$ ). These results imply that full transcriptional activation of ER $\alpha$  is dependent upon pSer294.

#### Phosphorylation of ER $\alpha$ on Ser294 is not promoted by growth factors

While our previous MS study focused on detection of ER $\alpha$  residues phosphorylated in response to E2, the influence of growth factors such as EGF upon ER $\alpha$  phosphorylation has never been investigated (18). To determine the status of Ser294 following growth factor stimulation, an optimized approach of on-bead trypsin digestion of ER $\alpha$  immunopurified from growth factor-treated MCF-7 cells followed by MRM/MS analysis was used. Quantitative assessment of relative changes in phosphorylation status was conducted by comparing the phosphorylated:unmodified peptide area ratio, the ratio of the MRM peak area of a phosphorylated peptide normalized to the peak area of its unmodified counterpart peptide. As a positive control, we analyzed ER $\alpha$  immunopurified from E2-treated as well as EGF-treated MCF-7 cells in a multiplexed MRM/MS assay which included quantitation of Ser167 phosphorylation as an internal control to confirm that our MRM/MS method could recapitulate the induction of Ser167 phosphorylation as determined by Western blot analysis using a well-validated pSer167 antibody. As the MRM/MS data shown in Fig. 2A and summarized graphically in Fig. 2B exhibit, treatment of serum-starved (NS) MCF-7 cells with EGF failed to provoke any detectable induction of Ser294 phosphorylation relative to control (Figs. 2A, top right, and B, left bar graph), whereas MRM/MS assessment of pSer167 within the same analysis revealed an 11-fold EGF induction of phosphorylation (Fig. 2A, bottom right, and B, right bar graph). The latter induction of pSer167 by EGF is a result consistent with numerous previous pSer167 antibody studies (26) and was confirmed by Western blot analysis of the immunopurified ER $\alpha$  (Fig. 2C). The 11-fold induction in pSer294 following E2 treatment (Fig. 2A, top left, and B, left bar graph) and

3.2-fold E2 inductions of pSer167 (Fig. 2A, bottom left, and B, right bar graph) in MCF-7 cells grown in charcoal-stripped media are consistent with previously reported results and confirm the validity of the MRM/MS analysis (27). Two additional growth factors, insulin and heregulin- $\beta$ , also failed to induce pSer294 but did upregulate pSer167 (Supplementary Fig. S1), underscoring the inability of growth factors to stimulate pSer294.

#### Stable isotope dilution-multiple reaction monitoring

To determine the phosphorylation occupancy level of both Ser167 and Ser294, we synthesized 4 heavy isotope-labeled peptides corresponding to the unmodified and phosphorylated forms of the Ser167 and Ser294 peptides. First, a standard curve was prepared and analyzed for each synthetic peptide (Supplementary Fig. S2A) to assess the linearity of response, LOD, and LOQ (Supplementary Fig. S2B) as described in the Materials and Methods. The LOQs were determined to range between 259 and 667 attomoles (on column) for the 4 peptides (Supplementary Fig. S2B). To determine the level of unmodified and phosphorylated Ser294 and Ser167 in MCF-7 cells using SID-MRM, we spiked in 25 fmol of each of the 4 synthetic, heavy isotope-labeled peptides after on-bead trypsin digestion of the immunopurified ER $\alpha$ . Because the immunoprecipitation procedure captures more than 98% of ER $\alpha$  (18), it is suitable for quantitative evaluation of absolute levels of ER $\alpha$ . Using this approach, it was determined that the total amount of ER $\alpha$  per  $10^6$  cells of MCF-7 is  $26 \pm 5$  (mean  $\pm$  SD) femtomoles based on the Ser294 peptide and  $16 \pm 6$  femtomoles based on the Ser167 peptide (Supplementary Fig. S2C) in untreated, serum-starved conditions. To determine the phosphorylation stoichiometry, or percentage of phosphorylation, of Ser294 and Ser167, we divided the molar amount of phosphorylated Ser167- or Ser294-containing peptide by the total amount of ER $\alpha$  (modified and unmodified). Under conditions of maximal phosphorylation, Ser294 was found to be 4% phosphorylated by E2 whereas Ser167 was 34% phosphorylated by EGF (Fig. 2D).

To confirm that Ser294 is more generally induced by E2 but not EGF in multiple breast cancer model systems, 2 other ER $\alpha$ -positive human breast cancer cell lines, BT474 and T47D, were analyzed in parallel with MCF-7. As shown in Fig. 3A, relative quantitation by MRM/MS of ER $\alpha$  immunopurified from these cell lines following EGF treatment revealed no induction of pSer294. In contrast, pSer294 was induced by E2 and, to a lesser extent, by 4-hydroxytamoxifen treatment (Fig. 3B).

#### Differential regulation of phosphorylation at ER $\alpha$ Ser294 and Ser305 by growth factors and E2

As Ser294 is situated in the hinge region of ER $\alpha$ , it was of interest to examine the phosphorylation status of the neighboring hinge region Ser305, as phosphorylation at this serine has been implicated as a breast cancer marker indicative of poor prognosis and resistance to tamoxifen (10, 11). While detection of peptides containing residue Ser305 by MS has proven difficult (18), the recent availability of a monoclonal

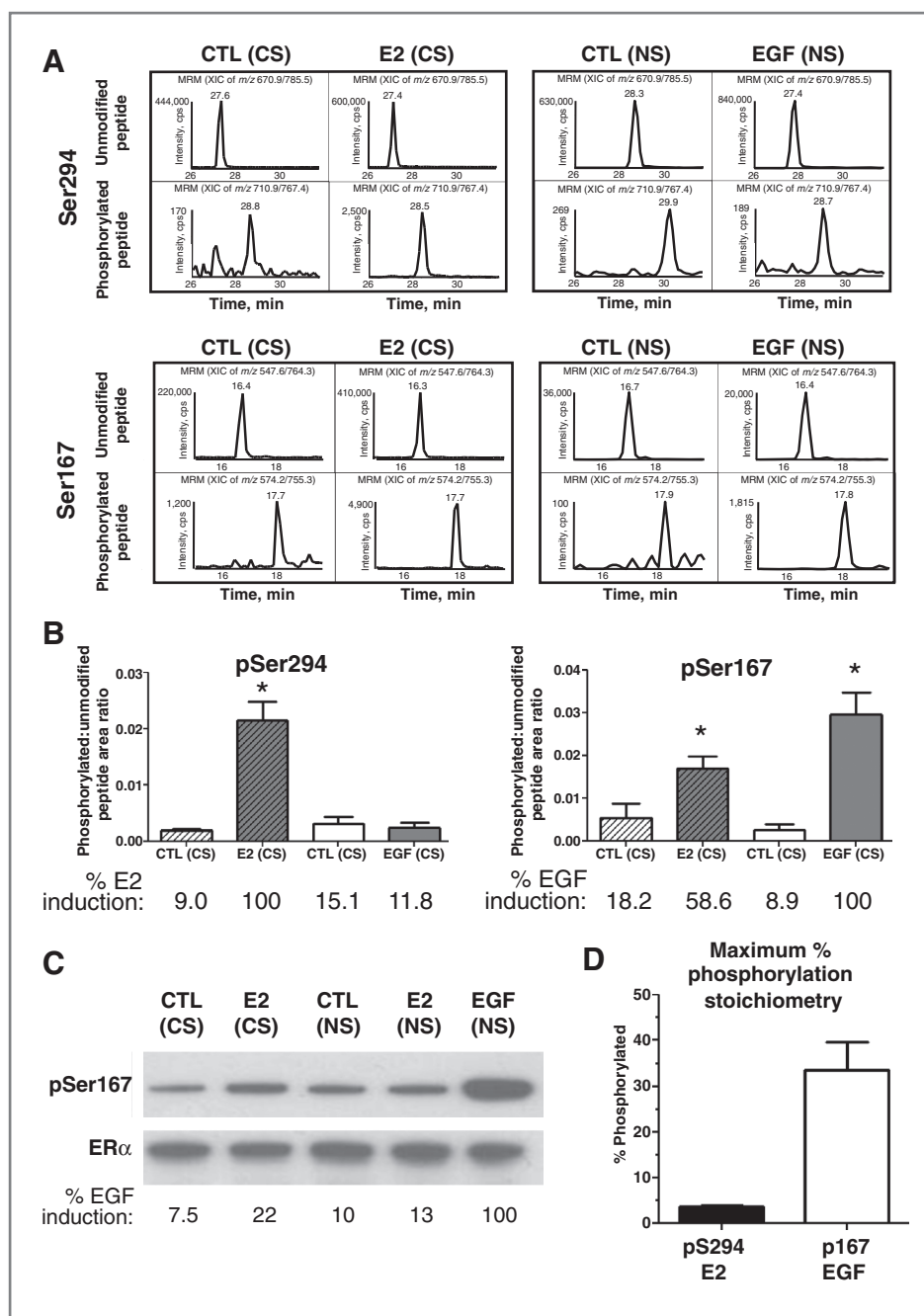


**Figure 2.** Phosphorylation of ER $\alpha$  Ser294 is induced by E2, but not EGF, in MCF-7 cells. **A**, MRM/MS assay chromatograms for the phosphorylated and unmodified Ser294 and Ser167 peptides from trypsin-digested ER $\alpha$  immunoprecipitates from MCF-7 cells. The MRM/MS transitions used to quantify the Ser294 peptide, 288-AANLWPSPLMIK-299, were Q1/Q3 670.9/785.5 corresponding to the  $[M+2H]^{2+}$  precursor and y7 fragment ion for the unmodified peptide and for the phosphorylated peptide Q1/Q3 710.9/767.4 was used corresponding to the  $[M+2H]^{2+}$  precursor and y7-98 fragment ion. The MRM transitions used to quantify the Ser167 peptide, 165-LASTNDKGSMMAMESAK-180, were Q1/Q3 547.6/764.3 corresponding to the  $[M+3H]^{3+}$  precursor and y15 $^{2+}$  for the unmodified peptide and for the phosphorylated peptide Q1/Q3 574.2/755.3 was used corresponding to the  $[M+3H]^{3+}$  precursor and y15 $^{2+}$ -49 fragment ion. MCF-7 cells were treated with 10 nmol/L E2 for 30 minutes or 8 nmol/L EGF for 10 minutes. For EGF treatment, cells were serum-starved (NS) for 24 hours before treatment, and for E2, cells were grown in charcoal-stripped (CS) media for 24 hours before treatment. **B**, MRM peak areas were used to calculate the phosphorylated:unmodified peptide area ratio, the relative MRM/MS peak areas of the phosphorylated 167 and 294 peptides normalized to the MRM/MS peak area of the unmodified peptide for each condition in **A**. Error bars represent the SD of at least 4 biologic replicates. \*, a significant difference ( $P < 0.05$ ) between the treatments and respective controls as assessed by the Student  $t$  test (2-way, unpaired). **C**, Western blot analysis of pSer167 levels induced following E2 and EGF treatments similar to those described in **A** confirm the concordance of Western blotting results with the MRM pSer167 induction results shown in **B**. Ser167 phosphorylation is induced by E2 in CS, but not NS, growth conditions. **D**, determination of the maximal stoichiometry of Ser294 and Ser167 phosphorylation using SID-MRM. The percentages of phosphorylation of Ser294 and Ser167 are maximal under E2 and EGF treatment, respectively, which are shown. Cells were grown in serum-free conditions for 24 hours. Error bars represent the SD of 2 independent biologic replicates.



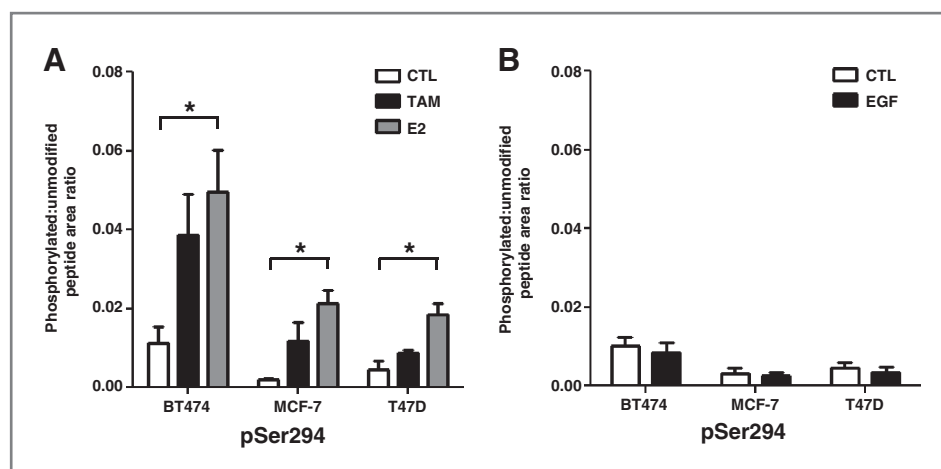


**Figure 3.** E2, but not EGF, induces phosphorylation of Ser294 in multiple cell lines. MRM/MS analysis of the induction of Ser294 phosphorylation by E2 and EGF in BT474, MCF-7, and T47D cell lines. A, in all cell lines, E2 induces Ser294 phosphorylation. B, EGF stimulation does not induce Ser294 phosphorylation in any cell line. Cells were treated with 8 nmol/L EGF for 10 minutes or 10 nmol/L E2 for 30 minutes. For EGF treatment, cells were serum-starved (NS) for 24 hours before treatment, and for E2, cells were grown in charcoal-stripped (CS) media for 24 hours before treatment. Error bars represent the SD of at least 3 biologic replicates. \*, a significant change ( $P < 0.05$ ) as assessed by the Student  $t$  test (2-way, unpaired). CTL, control; TAM, tamoxifen.

antibody to pSer305, which has supplanted the relatively ineffective pSer305 polyclonal antibodies, allowed for the quantitative determination of pSer305 by Western blot analysis on immunoprecipitated ER $\alpha$ . In addition, prompted by our initial MS findings on the selective induction of pSer294, we initiated development of an antibody specific for ER $\alpha$  pSer294 to independently validate our MS findings (Fig. 4A). To establish that Ser305 phosphorylation was preserved in the immunopurified ER $\alpha$  preparations, MCF-7 cells were treated with the protein kinase A (PKA) activator forskolin, as Ser305 phosphorylation has been reported to be directly mediated by PKA with forskolin stimulation of pSer305 in MCF-7 cells successfully validated using the pSer305 monoclonal antibody (10). As shown in Fig. 4A, pSer305 was induced by forskolin as well as by EGF but exhibited no induction following E2 stimulation, as expected, pSer294 was only induced by E2. Furthermore, while pSer118 and pSer167 were induced by EGF as expected, they were not induced by forskolin (Fig. 4A). We note that the results shown here showing the inability of E2 to induce pSer305 contradict several reports where pSer305 was detected following E2 stimulation in whole-cell lysates using a pSer305 polyclonal antibody (28, 29)

Given the diametrically opposing influences of E2 and growth factors in promoting pSer294 and pSer305, the consequence of co-stimulating with E2 and EGF were examined. Treating MCF-7 cells that had been serum-starved for 24 hours with a 20-minute stimulation of EGF, E2, or co-administration of both E2 and EGF (8 nmol/L EGF and 10 nmol/L E2) indicated that while Ser294 phosphorylation was slightly blunted by the EGF and E2 combination relative to E2 alone, induction of pSer305 by EGF was dramatically suppressed by co-stimulation with E2 (Fig. 4B). In response to decreasing doses of E2 (10, 2, or 0.2 nmol/L E2) in combination with 8 nmol/L EGF, a reciprocal dose-response was observed with a reduction in

pSer294 levels accompanied by increased pSer305 levels (Fig. 4B). In contrast, the robust EGF stimulation of pSer167, enhanced by E2 co-stimulation, remained relatively unaltered across the E2 titration spectrum (Fig. 4B). MRM/MS analysis of pSer294 and pSer167 confirmed these Western blotting results with E2 and EGF cotreatment producing a 32% suppression of Ser294 phosphorylation and a 70% phosphorylation increase in pSer167 induction compared with any signal-agent treatment (Fig. 4C).

#### CDKs phosphorylate ER $\alpha$ at Ser294

Because of the central role played by ER $\alpha$  in mediating many key signaling pathways, there has been considerable effort to determine the kinases promoting the site- and stimuli-specific phosphorylation of ER $\alpha$  (2, 26). With Ser294 positioned between 2 prolines (Pro-Ser-Pro), the kinase predictors Scansite (30) and NetPhosK (31) identified Ser294 as a potential CDK site. To test whether CDKs are capable of directly phosphorylating Ser294, we first conducted an *in vitro* kinase assay using recombinant CDKs 2, 4, 7, and 9 with recombinant ER $\alpha$  as substrate. As shown in Fig. 5A, pSer294 is phosphorylated maximally by CDK7 and to a lesser extent by CDKs 2, 4, and 9.

Having established that Ser294 was targeted by CDKs *in vitro*, the influence of CDKs upon pSer294 formation in MCF-7 cells was examined pharmacologically using a variety of well-established, CDK-selective small-molecule inhibitors as opposed to CDK siRNA approaches, as CDK protein downregulation can produce more complex phenotypic changes confounding experimental interpretation (19). Following 1 hour of pretreatment of MCF-7 cells with the different CDK small-molecule inhibitors, cells were E2 stimulated for an additional 30 minutes before ER $\alpha$  harvesting. As shown in Fig. 5B, pretreatment with the pan-CDK inhibitor, roscovitine at 50 and 5  $\mu$ mol/L, as well as pretreatment with the more selective CDK inhibitor

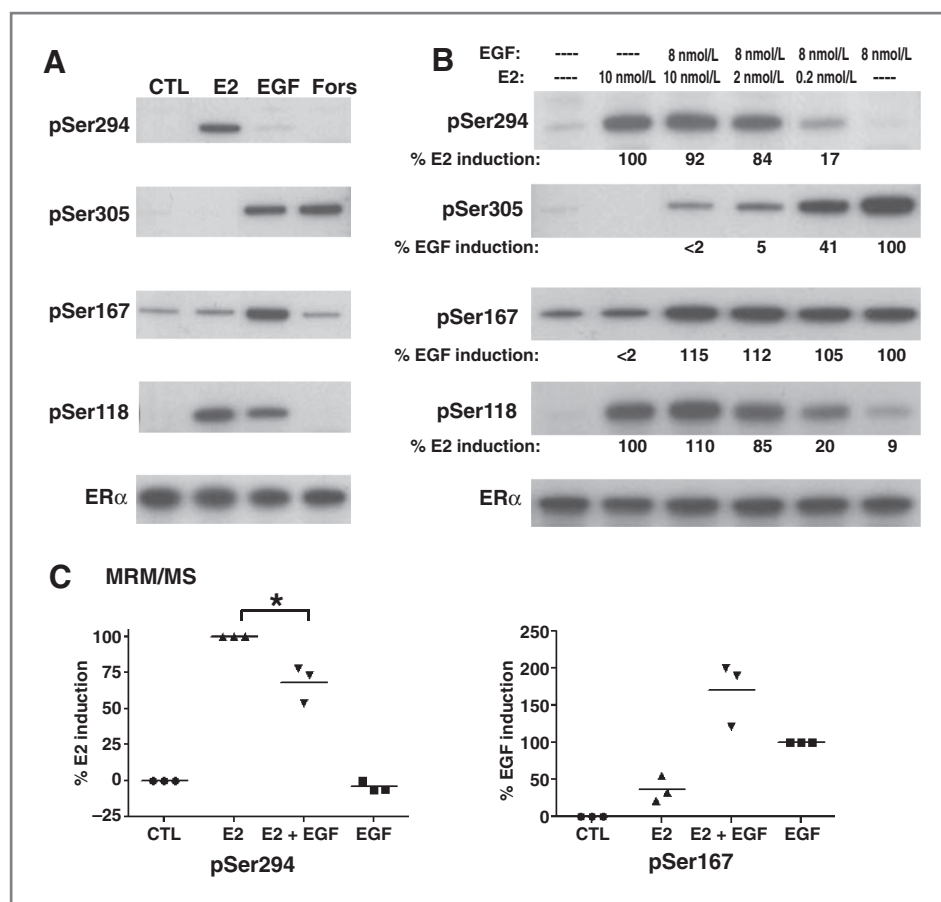


**Figure 4.** ER $\alpha$  hinge domain phosphorylation at Ser294 and Ser305 is suppressed by cross-talk between growth factor and ligand stimulation whereas N-terminal phosphorylation at pSer118 and pSer167 is enhanced. A, MCF-7 cells in serum-free conditions were either untreated (CTL), treated with E2 (10 nmol/L) for 30 minutes, EGF (8 nmol/L) for 14 minutes, or 10  $\mu$ mol/L forskolin (Fors) for 14 minutes. B, Western blot analysis of ER immunoprecipitated from MCF-7 cells either untreated (–), treated with EGF (8 nmol/L) for 20 minutes, treated with E2 (10 nmol/L) for 20 minutes, or cotreated with EGF (8 nmol/L) and E2 (10, 2, and 0.2 nmol/L) for 20 minutes. Total ER $\alpha$  served to normalize lane loading. C, MRM/MS analysis of immunoprecipitated/trypsin-digested ER from MCF-7 cells; untreated (CTL), E2 (10 nmol/L)-, EGF (8 nmol/L)-, and E2 + EGF (10 nmol/L E2, 8 nmol/L EGF)-treated samples shown in B with the MRM/MS peak area ratio used to determine the induction of Ser294 and Ser167 phosphorylation. Percentage of E2 induction of Ser294 and percentage of EGF induction of pSer167 are shown. \*, *P* value below 0.05 as assessed by the Student *t* test (2-way, unpaired).

SNS-032 (CDK 2, 7, and 9; ref. 32) at a low dose of 1  $\mu$ mol/L suppressed E2 induction of pSer294 by approximately 89% following roscovitine pretreatments and 52% following SNS-032 pretreatment relative to E2 treatment alone, as determined by MRM/MS analysis of immunopurified ER $\alpha$ . As roscovitine treatment had previously been used to show that E2 induction of pSer118 was not CDK-mediated (33), Western blot analysis was used to confirm that the CDK inhibitor treatments did not influence E2 induction of pSer118 as well as to validate the MRM/MS result for CDK inhibitor suppression of pSer294 induced by E2 (Fig. 5C). In addition, the availability of a rabbit monoclonal antibody to ER $\alpha$  pSer104/pSer106, 2 other AF-1 domain serines putatively targeted by CDKs (34), allowed examination of the CDK responsiveness of these sites. As shown in Fig. 5C, CDK inhibition produced no change in the slightly enhanced (vs. control) level of E2-induced pSer104/pSer106. These results strongly argue that following E2 stimulation, Ser294 is the primary CDK target on intracellular ER $\alpha$  among known phosphorylation sites.

## Discussion

The constellation of phosphorylated residues within the endogenous ER $\alpha$  of human breast cancers that functionally direct receptor conformation, protein–protein interactions,

and genomic activity also represent a posttranslational code reflecting the integration of ligand-dependent and -independent ER $\alpha$  activation signals (2, 6). Up to 50% of ER-positive breast cancers exhibit endocrine resistance to ligand-targeted therapeutics, yet retain some dependence on the growth promoting genomic ( $\pm$ nongenomic) activity of activated ER $\alpha$ . As a result, clinical investigators continue to evaluate the combination of standard endocrine agents with various small-molecule inhibitors of protein kinase cross-talking pathways presumed to target ER $\alpha$  and drive the ligand-independent growth and endocrine resistance of ER-positive breast cancers (3, 4). Despite compelling preclinical rationale for these therapeutic combinations, these clinical trials have been inconclusive due to the lack of validated biomarkers, other than the presence of ER $\alpha$  itself, which have the ability to predict endocrine sensitivity or point to specific protein kinases targeting ER $\alpha$  that may induce endocrine resistance. Ser118 and Ser167 were identified early on as AF-1 domain phosphorylation sites linked to ER $\alpha$  genomic activity and responsive to a multitude of different signaling kinases (2, 6). The clinical expectation was that phosphorylation at one or both of these AF-1 sites would identify endocrine-resistant breast cancers. However, the null or even opposite clinical findings correlating Ser118 and Ser167 phosphorylation with endocrine responsiveness (6–8) may now be understood in the light of the present

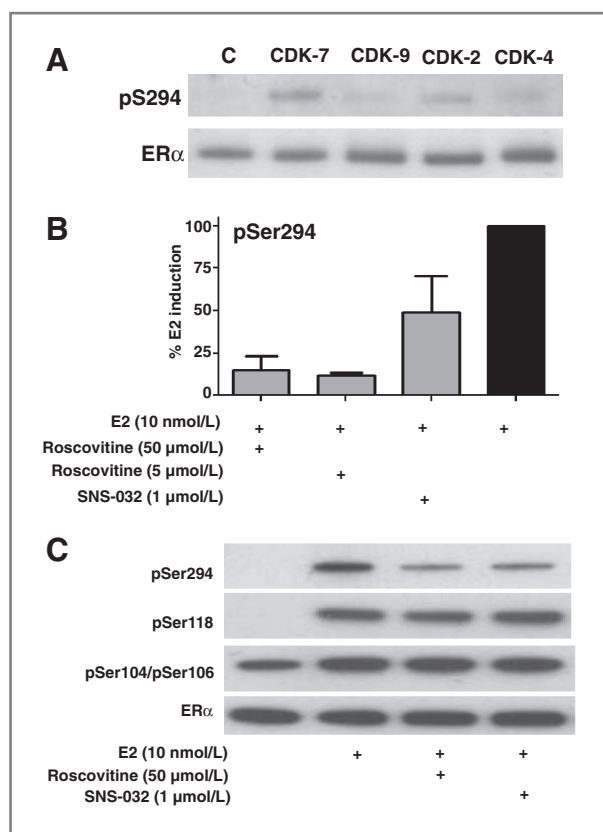


**Figure 5.** CDKs inhibit Ser294 phosphorylation *in vivo* and can phosphorylate Ser294 *in vitro*. **A**, *in vitro* phosphorylation of Ser294 CDKs, including CDKs 2, 4, 7, and 9 examined by Western blot analysis using pSer294 antibody. **B**, MRM/MS analysis of Ser294 phosphorylation of ER immunoprecipitated from MCF-7 cells treated with 10 nmol/L estradiol (E2) for 30 minutes or first pretreated for 1 hour with the broad-spectrum CDK inhibitors roscovitine (5 and 50  $\mu$ mol/L) or SNS-032 (1  $\mu$ mol/L) before E2 treatment. Both inhibitors decrease Ser294 phosphorylation relative to E2 alone (set equal to 100%). Error bars represent the SD for 3 biologic replicates. **C**, Western blot analysis of immunoprecipitated ER also showed a decrease in Ser294 phosphorylation following CDK inhibitor treatment using a pSer294 antibody. Western blot analysis of immunoprecipitated ER using antibodies to pSer118 and pSer104/pSer106 showed that inhibition of CDKs does not reduce their induction by E2. Equal ER loading is confirmed by probing for ER $\alpha$ .

study, which compares ER $\alpha$  hinge and AF-1 domain phosphorylation responses in ER-positive breast cancer cells exposed to ligands, growth factors, or a combination of ligand-dependent and -independent cell stimuli. From these findings, it is clear that either ER ligands or growth factors can induce AF-1 (Ser118, Ser167) phosphorylation and that this phosphorylation is enhanced by the combination of these ER $\alpha$  stimuli compared with either stimulus alone. Thus, it is mechanistically unlikely that Ser118 or Ser167 phosphorylation status can discriminate between ligand-dependent and -independent ER $\alpha$  activation, let alone point to specific protein kinases involved in ligand-independent receptor cross-talk. In contrast, as we show here, the phosphorylation status of neighboring hinge domain sites at Ser294 and Ser305 is capable of

differentiating between ligand-dependent and -independent ER $\alpha$  activation.

Hinge domain phosphorylation at Ser305 was found within the past decade to be linked to 2 different protein kinases in an apparent ligand-independent manner (9, 10). The recent development of a monoclonal antibody specific to phosphorylated Ser305 enabled initial breast cancer biomarker studies to claim that ER $\alpha$  phosphorylation at this site may correlate with antiestrogen resistance (11, 12). About this same time, and using an MRM/MS approach, we first identified the presence of another hinge domain phosphorylation site at Ser294 expressed in ligand (E2)-stimulated MCF-7 cells (18). As illustrated here using a quantitative MRM/MS approach, ER $\alpha$  phosphorylation at Ser294 occurs in a variety of breast cancer cell lines (MCF-7, T47D, BT474) following E2 stimulation. The fact that a partially agonistic ligand such as 4-hydroxytamoxifen is also capable of inducing pSer294, but to a lesser extent than the fully agonistic E2 ligand, indicates that this hinge phosphorylation response does not depend on a specific change in ER $\alpha$  helix 12 conformation within the C-terminal ligand-binding domain. During the course of our MRM/MS studies, we developed a polyclonal rabbit antisera capable of specifically detecting ER $\alpha$  phosphorylation at Ser294 in ER $\alpha$ -immunoprecipitated samples, enabling independent validation of our MRM/MS results by Western blotting. Using both MRM/MS and immunoblotting approaches, we evaluated immunoprecipitated ER $\alpha$  from cells exposed to various growth factor (EGF, insulin, heregulin- $\beta$ ) stimuli, finding none that could induce Ser294 phosphorylation, although they were fully capable of inducing phosphorylation at Ser118 and Ser167 in the AF-1 domain and at the neighboring hinge Ser305 site. Therefore, the unique ability of Ser294 to respond only to ligand stimuli sets it apart from all other known ER $\alpha$  phosphorylation sites and enables it to serve as a specific readout for ligand-dependent ER $\alpha$  activation. In addition, the dominant-negative experiments shown in Fig. 1 using an ER $\alpha$  expression construct mutated at Ser294 reinforces previous results (20) suggesting that phosphorylation at Ser294 is required for ER $\alpha$  to promote full ligand-induced transcriptional activity.

To test the use of using both Ser294 and Ser305 phosphorylation as companion readouts to distinguish ligand-dependent from -independent ER $\alpha$  activation, we costimulated cells with EGF (8 nmol/L) and varying physiologic concentrations of E2 (0.2, 2.0, and 10 nmol/L) and then compared the hinge phosphorylation responses with those produced by ligand or growth factor stimulation alone. While EGF appeared to blunt E2-induced Ser294 phosphorylation by  $\leq 20\%$  compared with E2 alone, increasing doses of E2 caused progressively greater suppression of EGF-induced Ser305 phosphorylation, reaching more than 98% suppression at 10 nmol/L E2 relative to EGF alone. Because cell exposure to 10 nmol/L E2 or 8 nmol/L EGF maximally stimulated Ser294 and Ser305 phosphorylation respectively, the mild suppression of Ser294 phosphorylation by EGF and the profound suppression of Ser305 phosphorylation by E2 are not simply consequences of inadequate receptor

stimulation by either ligand or growth factor. It is also noteworthy that when using the CDK inhibitor roscovitine to suppress E2-induced Ser294 phosphorylation, the corresponding E2-induced suppression of Ser305 phosphorylation was abated relative to E2 alone (data not shown). While future studies are needed to understand what enzymatic or protein-protein interactions mediate the apparent mutual exclusivity of phosphorylation events at neighboring Ser294 and Ser305 sites, these findings reinforce the conclusion that phosphorylation at these 2 hinge sites may be useful readouts to discriminate between ligand-dependent and -independent ER $\alpha$  activation, respectively.

Identification of the kinase-mediating E2 induction of pSer294 was of considerable interest both to expand understanding of ER $\alpha$  function and to provide future rationale for combining kinase inhibitors with endocrine therapeutics. Ser294 was the only 1 of 4 sites in ER $\alpha$  harboring a proline-directed kinase motif (Ser-Pro), for which the kinase responsible for phosphorylation remained unknown (2). Using a broadly active CDK inhibitor roscovitine, or a more selective CDK inhibitor, SNS-032, that targets CDKs 2, 7, and 9 (35), the E2 induction of pSer294 was suppressed by approximately 80% and 50%, respectively, relative to E2 stimulation alone. In contrast, simultaneous interrogation of other AF-1 phosphorylation sites confirmed an earlier report that E2 induction of pSer118 phosphorylation cannot be suppressed by roscovitine (33). Moreover, induction of Ser104 and Ser106 phosphorylation, 2 other potential CDK sites (34), was not inhibited by roscovitine. Therefore, Ser294 stands as the only CDK-mediated ER $\alpha$  phosphorylation site and, as such, likely plays a key role in the roscovitine-induced suppression of proliferation observed in tamoxifen-resistant breast cancer cells (36).

As our quantitative MRM/MS analyses indicated that nearly 5% of ER $\alpha$  is marked by Ser294 phosphorylation upon E2 binding and activation, it is noteworthy that this compares with the estimated amount of chromatin-bound ER $\alpha$  induced upon ligand stimulation of MCF-7 cells (37). Chromatin immunoprecipitation experiments have documented the ligand-dependent recruitment of ER $\alpha$  to gene promoters in conjunction with TFIID, a multiprotein transcription factor complex known to contain CDK7 (35, 37). In this regard, it is worthy to note that our CDK *in vitro* kinase assay clearly showed CDK7 as the CDK family member capable of promoting the most robust phosphorylation of ER $\alpha$  on Ser294. Along with the fact that our cellular E2 induction of Ser294 phosphorylation was measured under serum-free culture conditions in which the MCF-7 breast cancer cells are viable and transcribing but not actively dividing, these kinase studies led us to conclude that ligand-induced endogenous phosphorylation of Ser294 is mediated primarily by the transcription-regulating and cell-cycle-independent kinase, CDK7, a therapeutic target of current clinical interest whose expression appears to be significantly upregulated in breast cancers relative to matched normal breast tissues (GSE15852; ref. 38).

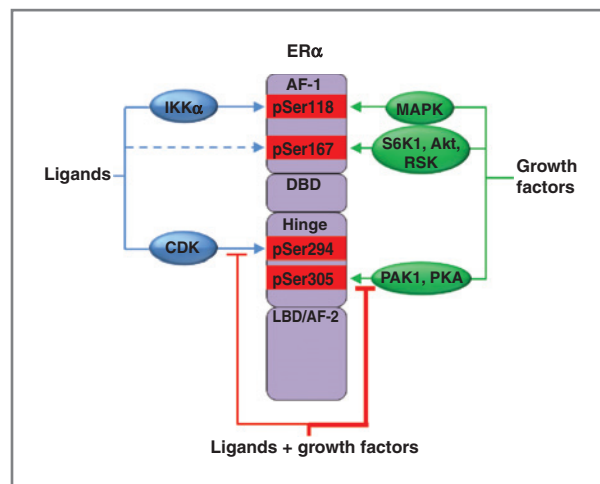


**Figure 6.** A model of ER $\alpha$  phosphorylation under ligand and growth factor stimuli. ER $\alpha$  (purple) consists of an AF-1, DNA-binding domain (DBD), hinge, and LBD/AF-2 domains. Ser118 phosphorylation is induced by both ligand (blue arrow) and growth factor stimulation (green arrow), whereas Ser167 phosphorylation is primarily induced by growth factors (green arrow) although weakly induced by ligand (dashed blue arrow). Kinases shown promoting pSer118 and pSer167 are not meant to exclude other AF-1 phosphorylating candidates; all candidate kinases as well as the indicated kinases promoting pSer305 are described in the work of Le Romancer and colleagues (2) except the ligand stimulation of pSer167 found in Britton and colleagues (27) and results shown in Fig. 2C. In the hinge domain, our study determined that Ser294 is phosphorylated by a CDK that is exclusively ligand-induced. Ser305 is induced only by growth factors. In contrast to the phosphorylation sites in the AF-1 domain which are co-stimulated by ligand and growth factors, hinge domain phosphorylation at Ser294 and Ser305 is suppressed by co-stimulation with ligand and growth factors (red lines) with the heavier red line to pSer305 relative to the thinner red line to pSer294 indicating the approximately 5-fold greater suppression of pSer305 relative to pSer294 at the co-stimulatory concentration of 10 nmol/L estrogen with 8 nmol/L EGF (see Fig. 4A). MAPK, mitogen-activated protein kinase.

In conclusion, key results are summarized schematically in the model diagram shown in Fig. 6. Here, hinge domain phosphorylations at Ser294 and Ser305 are represented as mutually exclusive ER $\alpha$  states, functionally distinct from AF-1 phosphorylation responses where both Ser118 and Ser167 phosphorylations are stimulated by ligand and growth factor treatment. Phosphorylation at Ser294 predominates upon ligand-induced receptor activation with this phosphorylation state becoming partially blunted by growth factor cotreatment. In contrast, phosphorylation at Ser305 is maximal under conditions of growth factor stimulation (cross-talk) but becomes rapidly suppressed as estrogen concentrations are increased. As inferred from the Western blotting of Fig. 4B, with estrogen and EGF concentrations at their standard 10 and 8 nmol/L levels, respectively, cotreatment produces at least 50-fold suppression of pSer305 levels relative to the EGF condition, whereas pSer294 levels are suppressed by less than approximately 10%. However, translating results from an *in vitro* model system into relevant *in vivo* clinical situations remain a challenge particularly when trying to understand how the various constellations of ER $\alpha$  phosphorylations might predict ER $\alpha$ -positive



breast cancer outcome and responsiveness to antiestrogenic therapy. In addition to a series of clinical studies using phospho-specific antibodies to evaluate pSer118, pSer167, and pSer305 as single markers of endocrine responsiveness (39), another report has shown significantly better outcome predictability when multiple phospho-specific antibodies directed against a suite of phosphorylated ER $\alpha$  sites (including those not shown in Fig. 6) are used (39, 40). While pSer294 was among the 7 different ER $\alpha$  phosphorylation sites evaluated in this latter analysis of more than 300-tamoxifen treated breast cancer cases, unfortunately, pSer305 was not evaluated (40). The recent commercial availability of a pSer305 antibody and our current development of a more robust rabbit monoclonal directed at ER $\alpha$  pSer294 offer a future opportunity to show that hinge phosphorylation at Ser294 and Ser305 may be sufficient to discriminate endocrine-sensitive from endocrine-resistant breast cancers. It is also possible that rapidly evolving MS technologies will provide even greater clinical predictive power over standard immunohistochemical or other antibody-based ER $\alpha$  assays. While the sensitivity of antibodies to interrogate thin slices of fixed tissue for a single epitope would be difficult to match using current MS methods, the ability of MS to conduct global proteomic analysis and to interrogate the stoichiometry of ER $\alpha$  phosphorylation at either one specific residue of interest or across multiple phosphorylation sites within the same ER $\alpha$  peptide region offer better PTM definition and potentially improved clinical predictive use over that achievable by any current immunoassays.

## References

1. Deroo BJ, Korach KS. Estrogen receptors and human disease. *J Clin Invest* 2006;116:561–70.
2. Le Romancer M, Poulard C, Cohen P, Sentis S, Renoir JM, Corbo L. Cracking the estrogen receptor's posttranslational code in breast tumors. *Endocr Rev* 2011;32:597–622.
3. Osborne CK, Schiff R. Mechanisms of endocrine resistance in breast cancer. *Annu Rev Med* 2011;62:233–47.
4. Miller TW, Balko JM, Arteaga CL. Phosphatidylinositol 3-kinase and antiestrogen resistance in breast cancer. *J Clin Oncol* 2011;29:4452–61.
5. Weigel NL, Moore NL. Steroid receptor phosphorylation: a key modulator of multiple receptor functions. *Mol Endocrinol* 2007;21:2311–9.
6. Murphy LC, Seekallu SV, Watson PH. Clinical significance of estrogen receptor phosphorylation. *Endocr Relat Cancer* 2011;18:R1–14.
7. Jiang J, Sarwar N, Peston D, Kulinskaya E, Shousha S, Coombes RC, et al. Phosphorylation of estrogen receptor- $\alpha$  at Ser167 is indicative of longer disease-free and overall survival in breast cancer patients. *Clin Cancer Res* 2007;13:5769–76.
8. Murphy LC, Skliris GP, Rowan BG, Al-Dhaheer M, Williams C, Penner C, et al. The relevance of phosphorylated forms of estrogen receptor in human breast cancer *in vivo*. *J Steroid Biochem Mol Biol* 2009;114:90–5.
9. Wang RA, Mazumdar A, Vadlamudi RK, Kumar R. P21-activated kinase-1 phosphorylates and transactivates estrogen receptor- $\alpha$  and promotes hyperplasia in mammary epithelium. *EMBO J* 2002;21:5437–47.
10. Michalides R, Griekspoor A, Balkenende A, Verwoerd D, Janssen L, Jalink K, et al. Tamoxifen resistance by a conformational arrest of the estrogen receptor  $\alpha$  after PKA activation in breast cancer. *Cancer Cell* 2004;5:597–605.
11. Holm C, Kok M, Michalides R, Fles R, Koonstra RH, Wesseling J, et al. Phosphorylation of the oestrogen receptor  $\alpha$  at serine 305 and prediction of tamoxifen resistance in breast cancer. *J Pathol* 2009;217:372–9.
12. Kok M, Zwart W, Holm C, Fles R, Hauptmann M, Van't Veer LJ, et al. PKA-induced phosphorylation of ER $\alpha$  at serine 305 and high PAK1 levels is associated with sensitivity to tamoxifen in ER-positive breast cancer. *Breast Cancer Res Treat* 2011;125:1–12.
13. Zwart W, de Leeuw R, Rondaj M, Neeffjes J, Mancini MA, Michalides R. The hinge region of the human estrogen receptor determines functional synergy between AF-1 and AF-2 in the quantitative response to estradiol and tamoxifen. *J Cell Sci* 2010;123:1253–61.
14. Wang C, Fu M, Angeletti RH, Siconolfi-Baez L, Reutens AT, Albanese C, et al. Direct acetylation of the estrogen receptor  $\alpha$  hinge region by p300 regulates transactivation and hormone sensitivity. *J Biol Chem* 2001;276:18375–83.
15. Berry NB, Fan M, Nephew KP. Estrogen receptor- $\alpha$  hinge-region lysines 302 and 303 regulate receptor degradation by the proteasome. *Mol Endocrinol* 2008;22:1535–51.
16. Sentis S, Le Romancer M, Bianchin C, Rostan MC, Corbo L. Sumoylation of the estrogen receptor  $\alpha$  hinge region regulates its transcriptional activity. *Mol Endocrinol* 2005;19:2671–84.
17. Subramanian K, Jia D, Kapoor-Vazirani P, Powell DR, Collins RE, Sharma D, et al. Regulation of estrogen receptor  $\alpha$  by the SET7 lysine methyltransferase. *Mol Cell* 2008;30:336–47.
18. Atsriku C, Britton DJ, Held JM, Schilling B, Scott GK, Gibson BW, et al. Systematic mapping of posttranslational modifications in human

## Disclosure of Potential Conflicts of Interest

D.J. Britton has employment (other than primary affiliation; e.g., consulting) in Proteome Sciences plc as Senior Research Scientist, has a commercial research grant from Proteome Sciences plc, and also has other commercial research support from Proteome Sciences plc. No potential conflicts of interest were disclosed by the other authors.

## Authors' Contributions

**Conception and design:** J.M. Held, G.K. Scott, B. Schilling, B.W. Gibson, C.C. Benz

**Development of methodology:** J.M. Held, D.J. Britton, G.K. Scott, M.A. Baldwin, B.W. Gibson, C.C. Benz

**Acquisition of data (provided animals, acquired and managed patients, provided facilities, etc.):** J.M. Held, D.J. Britton, E.L. Lee, B. Schilling

**Analysis and interpretation of data (e.g., statistical analysis, biostatistics, computational analysis):** J.M. Held, D.J. Britton, G.K. Scott, C.C. Benz

**Writing, review, and/or revision of the manuscript:** J.M. Held, D.J. Britton, G.K. Scott, B. Schilling, M.A. Baldwin, B.W. Gibson, C.C. Benz

**Administrative, technical, or material support (i.e., reporting or organizing data, constructing databases):** J.M. Held, D.J. Britton, C.C. Benz

**Study supervision:** J.M. Held, B.W. Gibson, C.C. Benz

## Acknowledgments

The authors thank Christina Yau for bioinformatic advice.

## Grant Support

This work was supported by NIH grant R01-CA071468, a research collaboration grant from Proteome Sciences plc (UK), and Hazel P. Munroe memorial funding to the Buck Institute (to C.C. Benz). The use of the 4000 QTRAP triple quadrupole/linear ion trap for MRM analysis was made possible by a shared instrumentation grant to the Buck Institute from the NCCR, S10 RR0021222 (to B.W. Gibson).

The costs of publication of this article were defrayed in part by the payment of page charges. This article must therefore be hereby marked *advertisement* in accordance with 18 U.S.C. Section 1734 solely to indicate this fact.

Received February 21, 2012; revised May 11, 2012; accepted June 1, 2012; published OnlineFirst June 5, 2012.

- estrogen receptor-alpha with emphasis on novel phosphorylation sites. *Mol Cell Proteomics* 2009;8:467–80.
19. Le Goff P, Montano MM, Schodin DJ, Katzenellenbogen BS. Phosphorylation of the human estrogen receptor. Identification of hormone-regulated sites and examination of their influence on transcriptional activity. *J Biol Chem* 1994;269:4458–66.
  20. Williams CC, Basu A, El-Gharbawy A, Carrier LM, Smith CL, Rowan BG. Identification of four novel phosphorylation sites in estrogen receptor alpha: impact on receptor-dependent gene expression and phosphorylation by protein kinase CK2. *BMC Biochem* 2009;10:36.
  21. Scott GK, Marx C, Berger CE, Saunders LR, Verdin E, Schafer S, et al. Destabilization of ERBB2 transcripts by targeting 3' untranslated region messenger RNA associated HuR and histone deacetylase-6. *Mol Cancer Res* 2008;6:1250–8.
  22. Addona TA, Abbatiello SE, Schilling B, Skates SJ, Mani DR, Bunk DM, et al. Multi-site assessment of the precision and reproducibility of multiple reaction monitoring-based measurements of proteins in plasma. *Nat Biotechnol* 2009;27:633–41.
  23. Nawaz Z, Lonard DM, Dennis AP, Smith CL, O'Malley BW. Proteasome-dependent degradation of the human estrogen receptor. *Proc Natl Acad Sci U S A* 1999;96:1858–62.
  24. Creighton CJ, Cordero KE, Larios JM, Miller RS, Johnson MD, Chinnaiyan AM, et al. Genes regulated by estrogen in breast tumor cells *in vitro* are similarly regulated *in vivo* in tumor xenografts and human breast tumors. *Genome Biol* 2006;7:R28.
  25. Britton DJ, Hutcheson IR, Knowlden JM, Barrow D, Giles M, McClelland RA, et al. Bidirectional cross talk between ERalpha and EGFR signalling pathways regulates tamoxifen-resistant growth. *Breast Cancer Res Treat* 2006;96:131–46.
  26. Lannigan DA. Estrogen receptor phosphorylation. *Steroids* 2003;68:1–9.
  27. Britton DJ, Scott GK, Schilling B, Atsriku C, Held JM, Gibson BW, et al. A novel serine phosphorylation site detected in the N-terminal domain of estrogen receptor isolated from human breast cancer cells. *J Am Soc Mass Spectrom* 2008;19:729–40.
  28. Al-Dhaheeri MH, Rowan BG. Protein kinase A exhibits selective modulation of estradiol-dependent transcription in breast cancer cells that is associated with decreased ligand binding, altered estrogen receptor alpha promoter interaction, and changes in receptor phosphorylation. *Mol Endocrinol* 2007;21:439–56.
  29. Giordano C, Cui Y, Barone I, Ando S, Mancini MA, Bero V, et al. Growth factor-induced resistance to tamoxifen is associated with a mutation of estrogen receptor alpha and its phosphorylation at serine 305. *Breast Cancer Res Treat* 2010;119:71–85.
  30. Obenauer JC, Cantley LC, Yaffe MB. Scansite 2.0: proteome-wide prediction of cell signaling interactions using short sequence motifs. *Nucleic Acids Res* 2003;31:3635–41.
  31. Blom N, Sicheritz-Ponten T, Gupta R, Gammeltoft S, Brunak S. Prediction of post-translational glycosylation and phosphorylation of proteins from the amino acid sequence. *Proteomics* 2004;4:1637–49.
  32. Chen R, Wierda WG, Chubb S, Hawtin RE, Fox JA, Keating MJ, et al. Mechanism of action of SNS-032, a novel cyclin-dependent kinase inhibitor, in chronic lymphocytic leukemia. *Blood* 2009;113:4637–45.
  33. Weitsman GE, Li L, Skliris GP, Davie JR, Ung K, Niu Y, et al. Estrogen receptor-alpha phosphorylated at Ser118 is present at the promoters of estrogen-regulated genes and is not altered due to HER-2 over-expression. *Cancer Res* 2006;66:10162–70.
  34. Rogatsky I, Trowbridge JM, Garabedian MJ. Potentiation of human estrogen receptor alpha transcriptional activation through phosphorylation of serines 104 and 106 by the cyclin A-CDK2 complex. *J Biol Chem* 1999;274:22296–302.
  35. Lapenna S, Giordano A. Cell cycle kinases as therapeutic targets for cancer. *Nat Rev Drug Discov* 2009;8:547–66.
  36. Nair BC, Vallabhaneni S, Tekmal RR, Vadlamudi RK. Roscovitine confers tumor suppressive effect on therapy-resistant breast tumor cells. *Breast Cancer Res* 2011;13:R80.
  37. Welboren WJ, van Driel MA, Janssen-Megens EM, van Heeringen SJ, Sweep FC, Span PN, et al. ChIP-Seq of ERalpha and RNA polymerase II defines genes differentially responding to ligands. *EMBO J* 2009;28:1418–28.
  38. Wesierska-Gadek J, Kramer MP. The impact of multi-targeted cyclin-dependent kinase inhibition in breast cancer cells: clinical implications. *Expert Opin Investig Drugs* 2011;20:1611–28.
  39. Skliris GP, Nugent ZJ, Rowan BG, Penner CR, Watson PH, Murphy LC. A phosphorylation code for oestrogen receptor-alpha predicts clinical outcome to endocrine therapy in breast cancer. *Endocr Relat Cancer* 2010;17:589–97.
  40. Skliris GP, Rowan BG, Al-Dhaheeri M, Williams C, Troup S, Begic S, et al. Immunohistochemical validation of multiple phospho-specific epitopes for estrogen receptor alpha (ERalpha) in tissue microarrays of ERalpha positive human breast carcinomas. *Breast Cancer Res Treat* 2009;118:443–53.